Available online at www.sciencedirect.com
ScienceDirect
Journal of Environmental Sciences 2010, 22(9) 1327–1334
JOURNAL OF ENVIRONMENTAL SCIENCES
ISSN 1001-0742
CN 11-2629/X
www.jesc.ac.cn

Removal of humic acid from aqueous solution by cetylpyridinium bromide modified zeolite

Yanhui Zhan[1], Zhiliang Zhu[1,*], Jianwei Lin[2], Yanling Qiu[1], Jianfu Zhao[1]

1. State Key Laboratory of Pollution Control and Resource Reuse, Tongji University, Shanghai 200092, China. E-mail: zhanyanhuijw@126.com
2. College of Marine Science, Shanghai Ocean University, Shanghai 201306, China

Received 01 November 2009; revised 30 December 2009; accepted 14 January 2010

Abstract

Natural zeolite was modified by loading cetylpyridinium bromide (CPB) to create more efficient sites for humic acid (HA) adsorption. The natural and CPB modified zeolites were characterized with X-ray diffraction, field emission scanning electron microscopy, Fourier transform infrared spectroscopy and elemental analysis. The effects of various experimental parameters such as contact time, initial HA concentration, solution pH and coexistent Ca^{2+}, upon HA adsorption onto CPB modified zeolites were evaluated. The results showed that natural zeolite had negligible affinity for HA in aqueous solutions, but CPB modified zeolites exhibited high adsorption efficiency for HA. A higher CPB loading on natural zeolites exhibited a larger HA adsorption capacity. Acidic pH and coexistent Ca^{2+} were proved to be favorable for HA adsorption onto CPB modified zeolite. The kinetic process was well described by pseudo second-order model. The experimental isotherm data fitted well to Langmuir and Sips models. The maximum monolayer adsorption capacity of CPB modified zeolite with surfactant bilayer coverage was found to be 92.0 mg/g.

Key words: modified zeolite; cetylpyridinium bromide; humic acid
DOI: 10.1016/S1001-0742(09)60258-8

Introduction

Humic substances are universally present in natural waters and soils. They are not well-defined substances, but generally can be subdivided into humin, humic acids (HA) and fulvic acids (FA) based on their solubility under acidic or alkaline conditions in aqueous solutions. Humic substances can react with chlorine during drinking water treatment and produce disinfection byproducts (DBPs), such as trihalomethanes with potential adverse health impacts (Karnik et al., 2005; Wan Ngah et al., 2008). Thus, the removal of humic substances from water is necessary and many methods have been developed such as chemical coagulation, membrane separation, advanced oxidation and adsorption (Hartono et al., 2009; Karnik et al., 2005; Lowe and Hossain, 2008; Wan Ngah et al., 2008; Zhang et al., 2008). Among these methods, adsorption is generally regarded as a promising method and has been extensively studied for removal of humic substances. Various adsorbents, including activated carbon, unburned carbons, resin, chitosan, chitosan-coated granules, crosslinked chitosan-epichlorohydrin beads, Mg/Al layered double hydroxides, Mg/Fe layered double hydroxide, layer structured graphite oxide, amine-modified polyacrylamide-bentonite composite, surfactant-modified bentonite and irradiation-crosslinked carboxymethylchitosan, etc. have been tested for humic acid removal (Anirudhan and Ramachandran, 2007; Anirudhan et al., 2008; Daifullah et al., 2004; Gasser et al., 2008; Hartono et al., 2009; Vreysen and Maes, 2008; Wan Ngah et al., 2008; Wang et al., 2009; Zhang and Bai, 2003; Zhao et al., 2008).

Natural zeolites are crystalline microporous aluminosilicates with very well defined structures that consist of a framework formed by tetrahedrons of SiO_4 and AlO_4, and they possess permanent negative charge in their crystal structures that can be balanced by exchangeable cations such as Na^+, Ca^{2+}, K^+ and Mg^{2+} (Leyva-Ramos et al., 2008). Thus, natural zeolites usually can exchange cations but not anions, which making them suitable for surface modification using cationic surfactants, such as hexadecyltrimethylammonium bromide (HDTMA-Br) and cetylpyridinium bromide (CPB) (Chutia et al., 2009; Covarrubias et al., 2008; Ghiaci et al., 2004; Jin et al., 2008; Leyva-Ramos et al., 2008; Li and Hong, 2009; Ozdemir et al., 2009; Simpson and Bowman, 2009; Yusof and Malek, 2009; Wang et al., 2006; Warchoł et al., 2006; Wingenfelder et al., 2006). Although extensive studies on performance of HDTMA modified zeolite in removing anionic and organic contaminants and the intercalation of HDTMA into zeolite have been conducted, there are few reports concerning the performance of CPB modified zeolite in removing humic acid and the intercalation of CPB into zeolite.

* Corresponding author. E-mail: zzl@tongji.edu.cn

By loading cationic surfactant CPB onto one kind of natural zeolite, a composite adsorbent was prepared and applied to the removal of humic acid from aqueous solution. The objectives of this work were to determine the adsorption efficiency of this CPB modified zeolite, and to evaluate the factors affecting the adsorption process. The possible adsorption mechanisms were also discussed.

1 Materials and methods

1.1 Materials

The natural zeolite used in this study was collected from Jinyun County, Zhejiang Province, China. Their chemical compositions are as follows (in mass): SiO_2 69.58%, Al_2O_3 12.20%, Na_2O 2.59%, CaO 2.59%, MgO 0.13%, K_2O 1.13%, Fe_2O_3 0.87%, others 10.91%. The particle size of natural zeolite is smaller than 0.18 mm. According to the reported methods (Chutia et al., 2009), the external cation exchange capacity (ECEC) of the natural zeolite was determined to be 166 mmol/kg. Humic acid was purchased from Aldrich Chemical Co., Ltd. Reagent grade cetylpyridinium bromide was supplied by Sinopharm Chemical Reagent Co., Ltd. Other chemical reagents used in this study, such as NaOH, HCl, $CaCl_2$, KBr, were analytical reagent grade, and also obtained from Sinopharm Chemical Reagent Co., Ltd.

1.2 Preparation of CPB modified zeolite

The CPB modified zeolites were prepared by dipping natural zeolite in CPB aqueous solutions. Different volumes (18–72 mL) of CPB solutions with initial concentration of 50 mmol/L were placed in a flask and 9 g of natural zeolite was added. The resulting suspensions were shaken at fixed temperature (40 ± 0.5)°C and 150 r/min for 48 hr, a time sufficient to reach adsorption equilibrium. After completion of reaction, solid-liquid separation was achieved by centrifugation at 4000 r/min for 20 min. The residual CPB concentration in solutions was determined using a TU-1901 UV/Vis spectrophotometer (Beijing Purkinje General Instrument Co., Ltd., China) at λ_{max} = 259 nm. The concentrations of K^+, Na^+, Ca^{2+}, and Mg^{2+} in solutions were determined by an Optima 2100 DV inductively coupled plasma atomic emission spectroscopy (ICP-AES) (PerkinElmer, USA). The solid was washed with distilled water repeatedly to remove superficially held CPB molecules, and then was dried at 50°C in an oven for 12 hr.

1.3 Characterization of natural and modified zeolites

Powder X-ray diffraction (XRD) patterns of natural and modified zeolites were obtained using an X'Pert PRO X-ray diffractometer with CuK_α radiation (PANalyitcal, the Netherlands) operating at 40 kV and 40 mA. The diffraction patterns were identified using high-score plus files. The surfaces of natural and modified zeolites were examined using a JSM-7500F field emission scanning electron microscopy (FE-SEM) (JEOL Ltd., Japan). Fourier transfer infrared (FT-IR) spectra were recorded on a Thermo Nicolet 5700 (Thermo Nicolet Corporation, USA) with a resolution of 2 cm^{-1} by using attenuated total reflectance (ATR) technique. The spectrum was scanned from 400–4000 cm^{-1}. The contents of carbon in natural and modified zeolites were determined by a Vario EL III CHNOS elemental analyzer (Elementar Analysensysteme GmbH, Germany).

1.4 HA adsorption

1.4.1 Kinetic study

Batch kinetic experiments were performed by mixing a fixed amount of absorbent (50 mg) with 250 mL HA solution of initial concentration of 10 mg/L in a series of conical flasks. The pH of HA solution was previously adjusted to 7.5 by adding 0.1 mmol/L of HCl or NaOH solution. The mixtures were covered and agitated in a shaker at a constant speed of 200 r/min and temperature of (30 ± 0.5)°C. After a certain period of stirring, the entire suspension was taken from a conical flask and solid-liquid separation was achieved by centrifugation at 4000 r/min for 20 min. The residual HA concentration in the solution was then determined using a TU-1901 UV/Vis spectrophotometer at λ_{max} = 254 nm.

1.4.2 Isotherm study

Isotherm study was conducted using batch equilibrium experiments. Absorbent 0.1 g was added into every conical flask with 250 mL of aqueous solution containing different HA concentrations. HA solutions were previously adjusted to pH 7.5. The mixtures were shaken at a constant temperature of (25 ± 0.5)°C and constant agitation rate 200 r/min using a shaker for 48 hr. The mixtures were then centrifuged at 4000 r/min for 20 min. The residual HA concentration was finally determined.

1.4.3 Effect of CPB loading on modified zeolite, solution pH, and coexistent ions

The effects of surfactant loading amounts, initial solution pH and coexistent Ca^{2+} on HA adsorption on CPB modified zeolite were investigated by equilibrium experiments in conical flasks, which contained 50 mg of absorbent and 250 mL of HA solution in every flask. For initial pH effect study, initial HA concentration was 10 mg/L, and HA solutions were adjusted to pH 6.5–9.5. For other studies, initial HA concentration was 20 mg/L, and HA solutions were adjusted to pH 7.5. The mixtures in conical flasks were shaken at a constant speed of 200 r/min for 48 hr. For coexistent Ca^{2+} effect studies, HA solutions were controlled at (30 ± 0.5)°C. For other studies, HA solutions were controlled at (25 ± 0.5)°C. After completion of reaction, suspensions were taken from conical flasks and solid-liquid separation was achieved by centrifugation at 4000 r/min for 20 min. The residual HA concentration was then determined.

2 Results and discussion

2.1 CPB loading onto natural zeolite

The result of CPB loading onto natural zeolite is

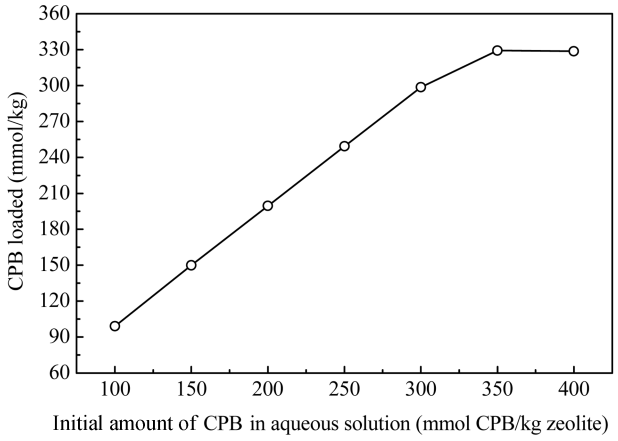

Fig. 1 CPB loading onto natural zeolite.

presented in Fig. 1. The amounts of CPB loaded onto natural zeolite depended on CPB available amounts in aqueous solutions (Fig. 1). The maximum CPB loading capacity of natural zeolite was 329 mmol/kg. The modified zeolites with CPB loading of 99, 149, 200, 249 and 329 mmol/kg were named as CPBZ1, CPBZ2, CPBZ3, CPBZ4 and CPBZ5, respectively.

2.1.1 XRD analysis

Figure 2 shows the XRD patterns of the natural zeolite and CPB modified zeolites. The crystalline species present in the zeolite material were identified comparing the characteristic peaks shown in the XRD pattern with the database of the diffractometer. It was found that the natural zeolite contained about 66% clinoptilolite, 19% mordenite and 15% quartz. The relative intensity of X-ray peaks corresponding to some typical crystallographic planes of the natural and modified zeolites are presented in Table 1. The structural parameters of the CPB modified zeolites are very close to that of corresponding parent zeolites, which indicate that the crystalline nature of the zeolites remained intact after chemical treatment with CPB molecules. It is also observed from Table 1 that the relative intensity of clinoptilolite characteristic peaks at 2θ of 9.97°, 11.31°, 17.47° and 25.76° were lessened, revealing that cation exchange reaction took place in the natural zeolites when they were treated by CPB solution.

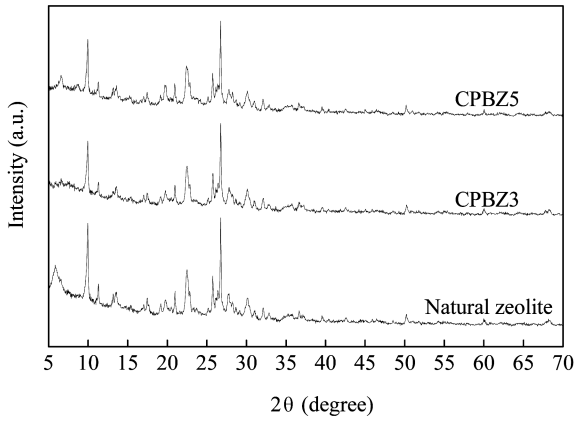

Fig. 2 XRD pattern of natural zeolite and CPB modified zeolites. CPBZ3 and CPBZ5 are modified zeolites with CPB loading of 200 and 329 mmol/kg, respectively).

2.1.2 FT-IR spectroscopy

The FT-IR spectra of crystalline CPB, natural zeolite and CPB modified zeolites are shown in Fig. 3. The following vibrations could be observed in the spectra of the crystalline CPB molecules: at 3401 cm^{-1} for O–H and N–H stretching bands, 3051 cm^{-1} and 1635 cm^{-1} for pyridine vibrations, 2916 cm^{-1} for C–H methylene asymmetric stretching band, 2850 cm^{-1} for C–H methylene symmetric stretching bands, 1479 cm^{-1} and 1388 cm^{-1} for aromatic C═C and aliphatic C–H stretching band, respectively. The FT-IR spectra of the CPB modified zeolites had additional two pronounced C–H bands (2800–3000 cm^{-1}) compared to that of the natural zeolite. The vibration bands at 2924 cm^{-1} (CPBZ1 and CPBZ2) and 2922 cm^{-1} (CPBZ3,

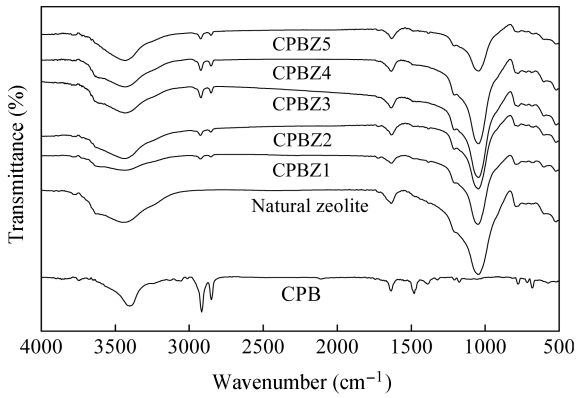

Fig. 3 FT-IR spectra of crystalline CPB, natural zeolite and CPB modified zeolites. CPBZ1–5 refer to Section 2.1.

Table 1 Typical X-ray peaks of natural zeolite and CPB modified zeolites

2θ (degree)	Natural zeolite		CPBZ3		CPBZ5	
	d (Å)	I/I_{max} (%)	d (Å)	I/I_{max} (%)	d (Å)	I/I_{max} (%)
9.97	8.87	76.1	8.88	60.3	8.88	63.8
11.31	7.83	19.6	7.82	15.9	7.84	17.0
17.47	5.08	15.0	5.06	10.7	5.08	12.5
20.98	4.23	23.3	4.24	22.6	4.24	23.6
22.46	3.96	44.6	3.96	45.4	3.97	43.6
25.76	3.46	41.1	3.46	39.3	3.46	38.3
26.75	3.33	100.0	3.33	100.0	3.33	100.0
27.73	3.22	23.1	3.21	23.5	3.21	20.9
30.19	2.96	20.5	2.97	22.8	2.97	19.8

d: interplanar spacing; I/I_{max}: relative intensity.

CPBZ4 and CPBZ5) are attributed to asymmetric CH_2 stretching vibration. The vibration bands at 2854 cm^{-1} (CPBZ1 and CPBZ2) and 2852 cm^{-1} (CPBZ3, CPBZ4 and CPBZ5) are attributed to symmetric CH_2 stretching vibration.

The frequencies and widths of the CH_2 stretching modes depend strongly on the conformation (or the *gauche/trans* conformer ratio) and the packing density of methylene chains (Rožić et al., 2009; Vaia et al., 1994). For the all-trans alkyl chain, such as crystalline CPB, the positions of CH_2 asymmetric and symmetric stretching modes are around 2916 and 2850 cm^{-1}, respectively (Fig. 3). If conformational disorder is included in the chains, their positions shift to higher wavenumber, depending upon the average content of gauche conformers (Rožić et al., 2009; Vaia et al., 1994). Small but observable differences in frequencies between the CPB modified zeolites and the crystalline CPB imply that CPB molecules on the modified zeolites have a more disordered structure than the crystalline CPB.

2.1.3 FE-SEM micrographs

The surfaces of the natural and modified zeolites were observed by using FE-SEM. This analysis revealed information about the details of the surface and morphology of the materials. The crystal structure of the natural zeolite can be seen clearly (Fig. 4a). The crystals with a tabular habit which is typical of clinoptilolite are observed in Fig. 4a. However, the crystal structure of the CPB modified zeolites shows different images. The crystal structures of CPBZ3 and CPBZ5 seem to be covered with a micellar surfactant surface coverage (Fig. 4b, c). This result indicates that an organic layer formed on the zeolite surface when natural zeolite was treated by CPB solution.

2.1.4 Elemental analysis

The contents of carbon in the natural and modified zeolites are shown in Table 2. The CPB modified zeolites had higher contents of carbon than the natural zeolite. In addition, a higher CPB loading on the natural zeolite resulted in a higher content of carbon. These results also confirm that CPB has been loaded onto natural zeolite after dipping in CPB solutions.

Table 2 Contents of carbon in natural zeolite and CPB modified zeolites

Samples	Carbon content (%)
Natural zeolite	0.0940
CPBZ1	2.92
CPBZ2	4.50
CPBZ3	6.03
CPBZ4	7.04
CPBZ5	8.61

2.1.5 Surfactant configuration on CPB modified zeolite

In order to evaluate surfactant configuration on the CPB modified zeolites, we determined the equivalent amounts of cations (K^+, Na^+, Ca^{2+} and Mg^{2+}) exchanged when the natural zeolites were treated by CPB solution. When CPB loaded amounts on the natural zeolite were 99, 149 and 200 mmol/kg, the total equivalent amounts of cations exchanged were 93, 126 and 143 mmol/kg, respectively. For CPBZ1, almost all of CPB molecules were bonded by electrostatic attraction, revealing that adsorbed CPB molecules formed a monolayer surface configuration. For CPBZ2, most of CPB (around 85%) were bonded by electrostatic attraction, and only a small part of CPB (around 15%) was bonded by hydrophobic interactions. This suggests that a majority of CPB molecules on CPBZ2 formed a monolayer surface configuration. For CPBZ3, its CPB loading level is much largerer than total equivalent amounts of cations exchanged. This means that adsorbed CPB molecules on CPBZ3 formed a patchy bilayer surface configuration. The CPB loading of CPBZ4 is much more than ECEC (166 mmol/kg) and less than twice of ECEC. This result indicates that adsorbed CPB molecules on CPBZ4 also formed a patchy bilayer surface configuration. The CPB loading of CPBZ5 is approximately twice as much as measured ECEC, indicating that adsorbed CPB molecules formed a bilayer surface configuration.

2.2 Adsorption capacity of HA on natural and modified zeolites

At initial HA concentration of 20 mg/L, the HA adsorption capacities on modified zeolites with different CPB loadings are shown in Fig. 5. The result showed that natural zeolite had a negligible affinity for HA in aqueous solutions. This may be due to the strong dipole interaction between natural zeolite and water, which excludes HA

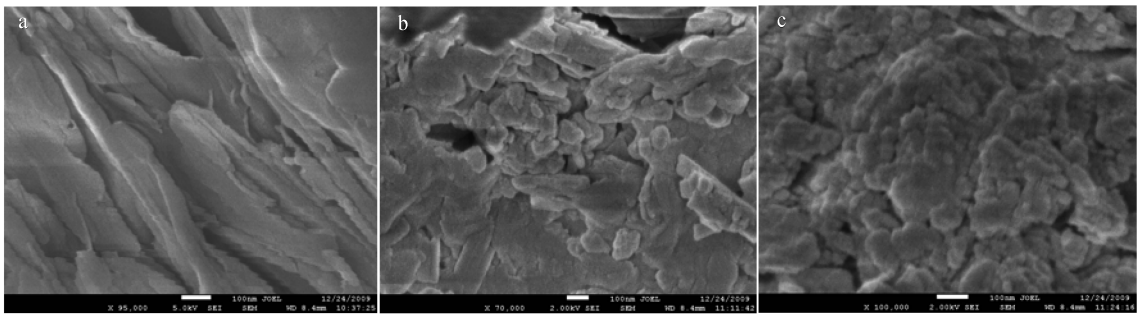

Fig. 4 FE-SEM photographs. (a) natural zeolite; (b) CPBZ3; (c) CPBZ5.

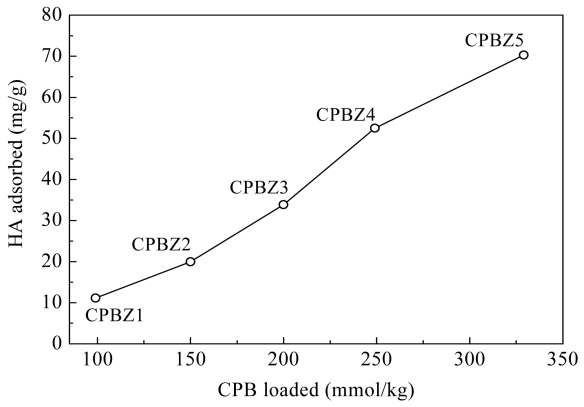

Fig. 5 HA adsorption capacity of modified zeolites with different CPB loadings.

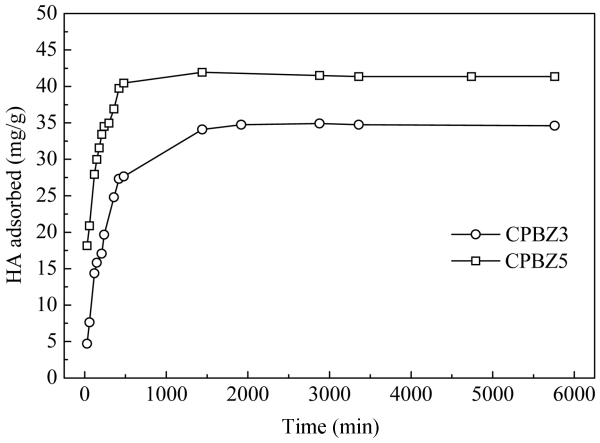

Fig. 6 Effects of contact time on HA adsorption onto CPB modified zeolites.

from zeolites (Wang et al., 2006). However, the CPB modified zeolites had a good affinity for HA in aqueous solution. Also, the CPB modified zeolite with higher surfactant loading amounts exhibited a better HA adsorption capacity. This result indicates that surface coverage as a bilayer rather than a monolayer or a patchy bilayer has a strongly favorable influence on HA adsorption onto CPB modified zeolites. Different mechanisms such as hydrophobic interaction, hydrogen bonding, and partitioning mechanism have been proposed to explain FA adsorption onto HDTMA modified zeolite with monolayer coverage (Wang et al., 2006). However, there are few studies on mechanism of HA adsorption onto CPB modified zeolite in previous literatures. It is well known that humic acid contains several kinds of functional groups, such as –COOH and –OH (Hartono et al., 2009). The formation of hydrogen bonds between N of CPB and hydroxyl groups and carboxylic groups of HA may be favorable to HA adsorption onto CPB modified zeolite. Koopal et al. (2004) found that a binding of cationic surfactant cetylpyridinium chlorine to HA was due to electrostatic and hydrophobic attractions. This indicates that hydrophobic interaction or electrostatic attraction may play an important role in HA adsorption onto CPB modified zeolite. Based on above discussions, some mechanisms such as hydrophobic interaction, hydrogen bonding and electrostatic attraction can be suggested to explain HA adsorption onto CPB modified zeolite. As a surfactant monolayer existed on CPB modified zeolite, HA adsorption may be attributed to hydrophobic interaction and hydrogen bonding. As a bilayer or patchy bilayer coverage existed on CPB modified zeolite, HA adsorption may be driven by a collaboration of hydrophobic interaction, hydrogen bonding and electrostatic interaction.

2.3 HA adsorption kinetics

The HA adsorption kinetics on CPBZ3 ad CPBZ5 were studied using initial HA concentration of 10 mg/L. As shown in Fig. 6, CPBZ5 exhibited much higher adsorption capacity than CPBZ3. This is in good agreement with findings from Fig. 5. The HA adsorption capacity of CPBZ3 or CPBZ5 also increased with increasing contact time (Fig. 6). Two commonly used kinetic models, pseudo first-order and second-order kinetic models have been applied to describe the adsorption of HA onto CPB modified zeolite as a function of contact time. The pseudo first-order kinetic model is expressed as below (Wang et al., 2009):

$$\ln(q_e - q_t) = \ln q_e - k_1 t \tag{1}$$

where, q_t (mg/g) and q_e (mg/g) represent the amount of adsorbate adsorbed at time t and at equilibrium time, respectively, and k_1 (min^{-1}) represents the adsorption rate constant. The adsorption rate constant (k_1) was calculated from the plot of $\ln(q_e - q_t)$ against t. The pseudo second-order kinetic model can be expressed as below (Wang et al., 2009):

$$\frac{t}{q_t} = \frac{1}{k_2 q_e^2} + \frac{t}{q_e} \tag{2}$$

where, k_2 (g/(mg·min)) is the pseudo second-order rate constant of sorption, q_e (mg/g) is the amount of adsorbate sorbed at equilibrium and q_t (mg/g) is the amount of adsorbate on the surface of the adsorbent at any time t. The q_e and k_2 can be obtained by linear plot of t/q_t versus t.

According to the calculated kinetic parameters shown in Table 3, it can be concluded that the pseudo second-order kinetic model can produce better fitting to the experimental data of HA adsorption. The result revealed that the chemisorption is significant in the rate controlling step.

2.4 HA adsorption isotherm

Figure 7 shows the experimental adsorption isotherms of HA onto CPBZ3 and CPBZ5. The HA adsorption capacity of CPB modified zeolite increased with increasing initial HA concentrations. This is due to the increment of the mass driving force which allows more HA molecules to pass from the aqueous solution to the adsorbent surface. It was also found that CPBZ5 exhibited much higher adsorption capacity than CPBZ3. Three kinds of adsorption isotherms, including Langmuir, Freundlich and Sips isotherm models, have been applied to describe experimental results. The Langmuir, Freundlich and Sips isotherm models are presented as Eqs. (3), (4) and (5), respectively

Table 3 Parameters and coefficients of kinetic models for HA adsorption onto CPB modified zeolite

Absorbent	$q_{e,exp}$ (mg/g)	Pseudo first-order model			Pseudo second-order model		
		k_1 (min^{-1})	q_e (mg/g)	R^2	k_2 (g/(mg·min))	q_e (mg/g)	R^2
CPBZ3	34.9	0.00325	32.6	0.988	0.000163	36.2	0.999
CPBZ5	41.9	0.00585	30.1	0.964	0.000549	41.8	0.999

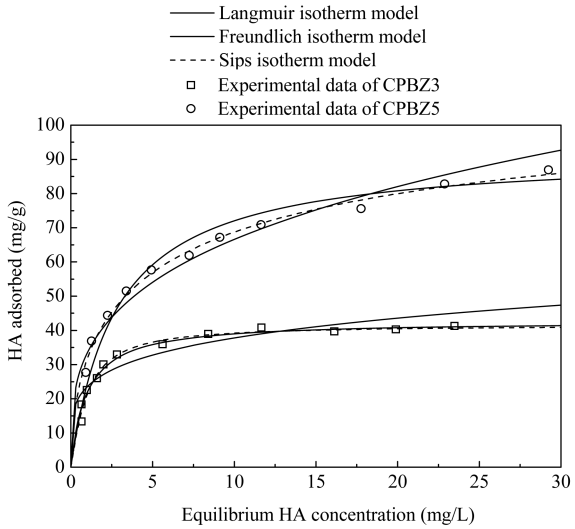

Fig. 7 Adsorption isotherm of HA onto CPB modified zeolites fitted to Langmuir model, Freundlich model, and Sips model.

(Hartono et al., 2009):

$$q_e = \frac{K_L q_m C_e}{1 + K_L C_e} \tag{3}$$

$$q_e = K_F C_e^{1/n} \tag{4}$$

$$q_e = \frac{q_m (K_L C_e)^{1/n}}{1 + (K_L C_e)^{1/n}} \tag{5}$$

where, K_L (L/mg) is the Langmuir adsorption constant related to the energy of adsorption, q_m (mg/g) is the maximum adsorption capacity, C_e (mg/L) is the equilibrium concentration and q_e (mg/g) is the equilibrium adsorption capacity, K_F (L/mg) is the Freundlich constant, and $1/n$ is the heterogeneity factor. The linearized form of Langmuir isotherm model is given as Eq. (6):

$$\frac{C_e}{q_e} = \frac{C_e}{q_m} + \frac{1}{K_L q_m} \tag{6}$$

The Langmuir constants K_L and q_m can be determined from the linear plot of C_e/q_e versus C_e. The linearized form of Freundlich isotherm model is given as Eq. (7):

$$\ln q_e = \ln K_F + \frac{1}{n} \ln C_e \tag{7}$$

The Freundlich constants K_F and $1/n$ are determined from the linear plot of $\ln q_e$ versus $\ln C_e$. The Sips constants K_L, q_m and $1/n$ are calculated based on Eq. (5) by nonlinear regression method. The isotherms of HA adsorption onto CPBZ3 and CPBZ5 predicted from above three models are plotted in Fig. 7. All the correlation coefficient, R^2 values and the constants obtained for the models are summarized in Table 4. The results show that three studied isotherm models have good fitting to the experimental results for HA adsorption on CPBZ5, and the Langmuir and Sips isotherm models produce slightly better fitting than the Freundlich isotherm model. Based on the Langmuir isotherm model, the maximum capacities of HA adsorption onto CPBZ3 and CPBZ5 are 42.5 and 92.0 mg/g, respectively (Table 4). Since Langmuir and Sips isotherm models are founded on the basis of homogenous surface, while Freundlich isotherm model promises to be applied to adsorption process occurred on heterogeneous surface, we deduced that the CPB modified zeolite might be mainly of surface energy homogeneity.

2.5 Effect of pH on HA adsorption onto CPB modified zeolite

The effect of initial solution pH on HA adsorption onto CPB modified zeolites was investigated. As shown in Fig. 8, the increment of initial solution pH resulted in a decrease in HA adsorption onto CPB modified zeolites. Furthermore, for different CPB loading amounts on zeolite, the increment in the initial solution pH produced different negative effects on HA adsorption efficiency. At initial HA solution concentration of 10 mg/L, an increase of initial

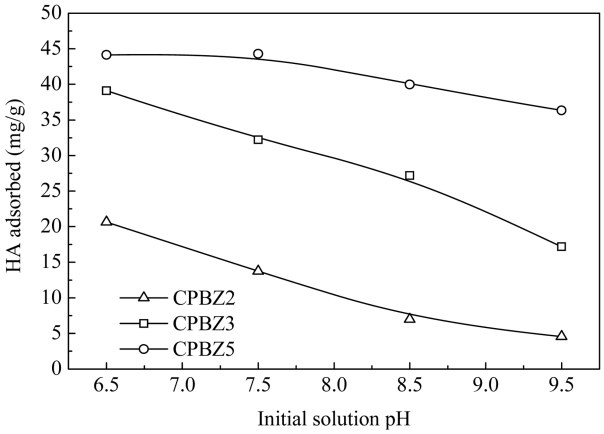

Fig. 8 Effects of initial solution pH on HA adsorption onto CPB modified zeolites.

Table 4 Isotherm constants for adsorption of HA on CPB modified zeolites

Adsorbent	Langmuir isotherm			Freundlich isotherm			Sips isotherm			
	q_m (mg/g)	K_L (L/mg)	R^2	K_F	$1/n$	R^2	q_m (mg/g)	K_L (L/mg)	$1/n$	R^2
CPBZ3	42.5	1.15	0.999	23.5	0.206	0.894	41.5	1.06	1.20	0.979
CPBZ5	92.0	0.360	0.994	33.3	0.301	0.964	121	0.162	0.567	0.993

solution pH from 6.5 to 9.5 decreased HA adsorption capacity of CPBZ2 from 20.6 to 4.6 mg/g and that of CPBZ3 from 39.1 to 17.2 mg/g, while the HA adsorption capacity of CPBZ5 only slightly decreased from 44.1 to 36.4 mg/g.

As discussed in earlier reports, hydrophobic interaction and hydrogen bonding may be important mechanisms for HA adsorption onto CPB modified zeolite. The HA solution may be considered as mixture of compounds with weakly acidic functional groups. At lower pH conditions, most of weakly acidic functional groups in HA are in uncharged states, hence more absorbable. As pH value increases, the amount of undissociated HA molecules will decrease, but dissociated HA molecules will increase. The negatively charged HA molecules are difficult to be adsorbed by CPB modified zeolite with monolayer coverage. Therefore, it is expected that HA adsorption onto CPBZ2 markedly decreases as pH value increases from 6.5 to 9.5. The surface charge of CPB modified zeolite with bilayer coverage is positive, which will favor the adsorption of negative charge ions of HA. The undissociated HA molecules dominating at low pH will be adsorbed due to hydrophobic interaction and hydrogen bonding. At higher pH values, dissociated HA molecules will be adsorbed due to electrostatic attraction. Therefore, it can be anticipated that an increase in pH value from 6.5 to 9.5 results in a slight decrease of HA adsorption onto CPBZ5. The above results and discussions confirm that hydrophobic interaction and hydrogen bonding play important roles in HA adsorption onto CPB modified zeolite with monolayer coverage. The results also confirm that electrostatic interaction is an important factor for HA adsorption onto CPB modified zeolite with bilayer coverage in addition to hydrophobic interaction and hydrogen bonding.

2.6 Effect of Ca^{2+} onto HA adsorption

Table 5 shows the HA adsorption capacity of CPB modified zeolites at different Ca^{2+} concentrations. According to Table 5, coexisting Ca^{2+} was favorable for HA adsorption onto CPB modified zeolite. The electrostatic repulsion between free humic acid in aqueous solutions and adsorbed humic acid on the adsorbent material can be reduced by calcium ion bridging (Yoon et al., 1998), which is responsible for the enhancement of HA adsorption onto CPB modified zeolite by Ca^{2+}.

Table 5 Effect of Ca^{2+} on HA adsorption onto CPB modified zeolites

Absorbent	HA adsorbed (mg/g)	
	0 mg Ca^{2+}/L	40 mg Ca^{2+}/L
CPBZ2	18.64	46.68
CPBZ3	56.55	76.21
CPBZ5	77.48	83.39

3 Conclusions

Natural zeolite basically has little affinity to HA in aqueous solutions, but CPB modification can obviously change the adsorption characteristics of the zeolite for HA. The HA adsorption efficiency was found to be dependent on CPB loading amounts, initial HA concentration, contact time, solution pH and concentration of coexistent Ca^{2+}. A higher CPB loading amount on natural zeolite exhibited a better HA adsorption efficiency. Acidic pH was proved to be favorable for HA adsorption onto CPB modified zeolite. The kinetic process was well predicted by pseudo second-order model. The experimental isotherm data of HA adsorption onto CPB modified zeolite with a patchy bilayer or bilayer coverage were well fitted to Langmuir and Sips models. The maximum monolayer adsorption capacities of CPB modified zeolites with surfactant loadings of 200 mmol/kg and 329 mmol/kg were found as 42.5 mg/g and 92.0 mg/g, respectively. In addition, coexisting Ca^{2+} was favorable for HA adsorption onto CPB modified zeolite. This study indicates that CPB modified zeolite with a bilayer coverage is a potentially effective adsorbent for HA removal from aqueous solutions.

Acknowledgments

This work was supported by the National Major Project of Science & Technology Ministry of China (No. 2008ZX07421-002) and the National Natural Science Foundation of China (No. 50908142).

References

Anirudhan T S, Ramachandran M, 2007. Surfactant-modified bentonite as adsorbent for the removal of humic acid from wastewaters. *Applied Clay Science*, 35(3-4): 276–281.

Anirudhan T S, Suchithra P S, Rijith S, 2008. Amine-modified polyacrylamide-bentonite composite for the adsorption of humic acid in aqueous solutions. *Colloids and Surfaces A: Physicochemical and Engineering Aspects*, 326(3): 147–156.

Chutia P, Kato S, Kojima T, Satokawa S, 2009. Adsorption of As(V) on surfactant-modified natural zeolites. *Journal of Hazardous Material*, 162(1): 204–211.

Covarrubias C, Garcia R, Yanez J, Arriagada R, 2008. Preparation of CPB-modified FAU zeolite for the removal of tannery wastewater contaminants. *Journal of Porous Materials*, 15(4): 491–498.

Daifullah A A M, Girgis B S, Gad H M H, 2004. A study of the factors affecting the removal of humic acid by activated carbon prepared from biomass material. *Colloids and Surfaces A: Physicochemical and Engineering Aspects*, 235(1-3): 1–10.

Gasser M S, Mohsen H T, Aly H F, 2008. Humic acid adsorption onto Mg/Fe layered double hydroxide. *Colloids and Surfaces A: Physicochemical and Engineering Aspects*, 331(3): 195–201.

Ghiaci M, Abbaspur A, Kiaa R, Seyedeyn-Azad F, 2004. Equilibrium isotherm studies for the sorption of benzene, toluene, and phenol onto organo-zeolites and as-synthesized MCM-41. *Separation and Purification Technology*, 40(3): 217–229.

Hartono T, Wang S H, Ma Q, Zhu Z H, 2009. Layer structured graphite oxide as a novel adsorbent for humic acid removal from aqueous solution. *Journal of Colloid and Interface Science*, 333(1): 114–119.

Jin X Y, Jiang M Q, Shan X Q, Pei Z G, Chen Z L, 2008. Adsorption of methylene blue and orange II onto unmodified

and surfactant-modified zeolite. *Journal of Colloid and Interface Science*, 328(2): 243–247.

Karnik B S, Davies S H, Baumann M J, Masten S J, 2005. The effects of combined ozonation and filtration on disinfection by-product formation. *Water Research*, 39(13): 2839–2850.

Koopal L K, Goloub T P, Davis T A, 2004. Binding of ionic surfactants to purified humic acid. *Journal of Colloid and Interface Science*, 275(2): 360–367.

Leyva-Ramos R, Jacobo-Azuara A, Diaz-Flores P E, Guerrero-Coronado R M, Mendoza-Barron J, Berber-Mendoza M S, 2008. Adsorption of chromium(VI) from an aqueous solution on a surfactant-modified zeolite. *Colloids and Surfaces A: Physicochemical and Engineering Aspects*, 330(1): 35–41.

Li Z H, Hong H L, 2009. Retardation of chromate through packed columns of surfactant-modified zeolite. *Journal of Hazardous Materials*, 162(2-3): 1487–1493.

Lowe J, Hossain Md M, 2008. Application of ultrafiltration membranes for removal of humic acid from drinking water. *Desalination*, 218(1-3): 343–354.

Ozdemir O, Turan M, Turan A Z, Faki A, Enginc A B, 2009. Feasibility analysis of color removal from textile dyeing wastewater in a fixed-bed column system by surfactant-modified zeolite (SMZ). *Journal of Hazardous Materials*, 166(2-3): 647–654.

Rožić M, Ivanec Šipušić D, Sekovanić L, Miljanić S, Ćurković L, Hrenović J, 2009. Sorption phenomena of modification of clinoptilolite tuffs by surfactant cations. *Journal of Colloid and Interface Science*, 331(2): 295–301.

Simpson J A, Bowman R S, 2009. Nonequilibrium sorption and transport of volatile petroleum hydrocarbons in surfactant-modified zeolite. *Journal of Contaminant Hydrology*, 108(1-2): 1–11.

Vaia R A, Teukolsky R K, Giannelis E P, 1994. Interlayer structure and molecular environment of alkylammonium layered silicates. *Chemistry of Materials*, 6(7): 1017–1022.

Vreysen S, Maes A, 2008. Adsorption mechanism of humic and fulvic acid onto Mg/Al layered double hydroxides. *Applied Clay Science*, 38(3-4): 237–249.

Wang S G, Gong W X, Liu X W, Gao B Y, Yue Q Y, 2006. Removal of fulvic acids using the surfactant modified zeolite in a fixed-bed reactor. *Separation and Purification Technology*, 51(3): 367–373.

Wang S B, Ma Q, Zhu Z H, 2009. Characteristics of unburned carbons and their application for humic acid removal from water. *Fuel Processing Technology*, 90(3): 375–380.

Wan Ngah W S, Hanafiah M A K M, Yong S S, 2008. Adsorption of humic acid from aqueous solutions on crosslinked chitosan-pichlorohydrin beads: Kinetics and isotherm studies. *Colloids and Surfaces B: Biointerfaces*, 65(1): 18–24.

Warchoł J, Misaelides P, Petrus R, Zamboulis D, 2006. Preparation and application of organo-modified zeolitic material in the removal of chromates and iodides. *Journal of Hazardous Materials*, 137(3): 1410–1416.

Wingenfelder U, Furrer G, Schulin R, 2006. Sorption of antimonate by HDTMA-modified zeolite. *Microporous and Mesoporous Materials*, 95 (1-3): 265–271.

Yoon S H, Lee C H, Kim K J, Fane A G, 1998. Effect of calcium ion on the fouling of nanofilter by humic acid in drinking water production. *Water Research*, 32(7): 2180–2186.

Yusof A M, Malek N A, 2009. Removal of Cr(VI) and As(V) from aqueous solutions by HDTMA-modified zeolite Y. *Journal of Hazardous Materials*, 162(2-3): 1019–1024.

Zhang X, Bai R, 2003. Mechanisms and kinetics of humic acid adsorption onto chitosan-coated granules. *Journal of Colloid and Interface Science*, 264(1): 30–38.

Zhang P Y, Wu Z, Zhang G M, Zeng G M, Zhang H Y, Li J et al., 2008. Coagulation characteristics of polyaluminum chlorides PAC-Al30 on humic acid removal from water. *Separation and Purification Technology*, 63(3): 642–647.

Zhao L, Luo F, Wasikiewicz J M, Mitomo H, Nagasawa N, Yagi T et al., 2008. Adsorption of humic acid from aqueous solution onto irradiation-crosslinked carboxymethylchitosan. *Bioresource Technology*, 99(6): 1911–1917.